

EXPERIMENTAL AND CFD SIMULATION OF ROLL MOTION OF SHIP WITH BILGE KEEL

*Irkal Mohsin A.R., Indian Institute of Technology Madras, India.
S. Nallayarasu, Indian Institute of Technology Madras, India.
S.K. Bhattacharyya, Indian Institute of Technology Madras, India.*

ABSTRACT

Roll motion of ships and ship-like floating bodies is subject of interest since a long time. The roll motion and the related damping becomes highly unpredictable, unlike other motions. This is mainly due to the non-linear effects arising from the viscous flow around the hull and the appendages attached to it. Various roll motion mitigation devices such as U-tube tanks, active fins and bilge keel are used for stable operation of the ships. Out of these bilge keel turn out to be simple and economical roll damping devices.

KEYWORDS: Bilge keel, roll damping, CFD, vorticity.

NOMEMCLATURE

Abbreviations

CFD :Computational Fluid Dynamics
FAVOR :Fractional Area/Volume Obstacle Representation
FSRVM :Free Surface Random Vortex Method
GMO :General Moving Objects
NWT :Numerical Wave Tank
PIV :Particle Image Velocimetry
RAO :Response Amplitude Operator
Std.Dev. :Standard Deviation
VCG :Vertical Centre of Gravity
VOF :Volume Of Fluid

Notations

A Added mass moment of inertia co-efficient
 α Phase angle (rad)
 B Non-linear roll damping coefficient (N-ms²)
BM Metacentric radius (m)
 C Restoring moment in roll (N-m)
 δ Logarithmic decrement
 dT Time interval between successive roll peaks (s)
 ϵ Turbulent kinetic energy dissipation
 φ Roll angle (rad)
 φ_0 Initial heel angle (rad)
 $\dot{\varphi}$ Angular velocity (rad/s)
 $\ddot{\varphi}$ Angular acceleration (rad/s²)
GM Metacentric height (m)
H Wave height (cm)
 I Roll moment of inertia (kg-m²)
 k Turbulent kinetic energy

K_{xx} Roll radius of gyration (m)
KG Distance between keel and VCG (m)
L Wavelength of water wave (m)
 M_0 Maximum moment due to wave (N-m)
 T_n Roll natural period (s)
T Wave period (s)
t Instantaneous time (s)
 ζ Damping ratio

1. INTRODUCTION

The subject of roll damping is age old and has developed in the last few decades. The estimation of roll damping from empirical relations based on model tests gained popularity in the 1970's and 1980's. The total roll damping was divided into various components arising from viscous and non-viscous phenomenon of the flow around the hull. It is divided into hull skin friction, eddy component, lift and wave damping of naked hull; normal force damping, hull-pressure damping and wave-damping due to bilge keel (Ikeda et al. [1],[2],[3]; Schmitke[4], Himeno[5], Chakrabarti[6]). The various components are derived from simplified formulae obtained from related theory and model experiments. These empirical formulae were incorporated into various strip theory or potential flow based numerical solvers for prediction of roll motion of ships. Although this approach is widely used, the limitation of such method arises from the simplified derivations restricted to simple hull forms, appendages and other ship parameters. There is a continuous improvement in the empirical methods for prediction of roll damping and roll motion of ship with change in design of ships (Kawahara et al.[7]).

The use of bilge keel for roll damping has been studied by many ocean engineers and naval architects reported as early in 1900 by Bryan[8]. The effectiveness of bilge keel for various hull forms of ship was studied through experiments and numerical methods. In the last decade researchers have tried to revive the study on roll damping and bilge keel with the help of computational fluid dynamics (CFD) and other simplified numerical methods to account for viscosity effects. Roddier et al.[9] validated free surface random vortex method (FSRVM), 2D-code with his experiments of free floating cylinders fitted with bilge keel. FSRVM is a mesh-free code which solves the flow field by dividing it into irrotational and vortical flows. Seah and Yeung[10] validated the same 2D FSRVM code with the forced roll experiments of Na et al.[11]. Yu et al.[12] developed a 2D Navier-Stokes code to simulate the forced roll motion of FPSO section with bilge keel. Later Yu and Kinnas[13] used the same code to study various hull configurations under forced roll motion. Bangun et al.[14] developed a 2D Navier-Stokes code to study bilge keel of two widths (0.01 m and 0.02 m) and various orientations (0° , 10° , 20° , 45° , 60° and 90°) connected to a barge section under forced roll motion. Thiagrajan et al.[15] studied a FPSO model under forced roll motion fitted with bilge keel of various widths. FSRVM was used to simulate the experiments which show a good agreement. It was observed from all the mentioned literature that bilge keel improves roll damping and has a dependency on roll angle, orientation and position of attachment to the hull. The computational methods developed, predicted the roll damping closer to the experiments paving a way to a new approach in the field of roll damping. Also, further advancements in CFD and turbulence modeling have lead to the better simulation of such motions involving complex flow behaviors.

Hence, this paper attempts to make use of CFD in prediction of roll motion of a ship hull section with and without bilge keel under regular waves. A 1:100 scale, parallel middle body of a ship model is fabricated and attached with a frictionless bearing at its roll axis to allow a single degree of freedom roll under regular beam waves. The model experiments are carried out in a glass flume and the model is made to the width of the flume with a minimum gap so as to allow free roll motion. The measured roll response of the model without and with a bilge keel is used to validate the CFD simulations carried out in FLOW-3D code. FLOW-3D uses a fixed-mesh technique for simulating motion of bodies under fluid forces and moments. An attempt is made to understand the formation of vortices and their shedding from the bilge keel using CFD.

2. EXPERIMENTAL INVESTIGATION

2.1 TEST FACILITY

The experimental studies are restricted to the parallel middle body of a ship with rectangular midship section with bilge keel. The experimental investigation has been carried out using the scaled model in a flume in the Department of Ocean Engineering, IIT Madras which is 22 m in length, 0.6 m in width and 0.8 m in depth and has a piston type electro-mechanical wave-maker at one end. The wave flume is made of glass on all three sides to provide visual access for flow visualization experiments using PIV. The experimental set up in the glass flume is shown in Fig. 1. Regular waves with periods ranging from 0.75 s to 2 s and heights ranging from 1 cm to 10 cm can be generated in this flume. It has a beach on the end opposite to the wave-maker made up of perforated, fibre reinforced plastic curved plate so as to dissipate the waves and minimize reflection. The flume has the arrangement for fixing models to the side wall and also has a rail mounted platform for moving the models easily.

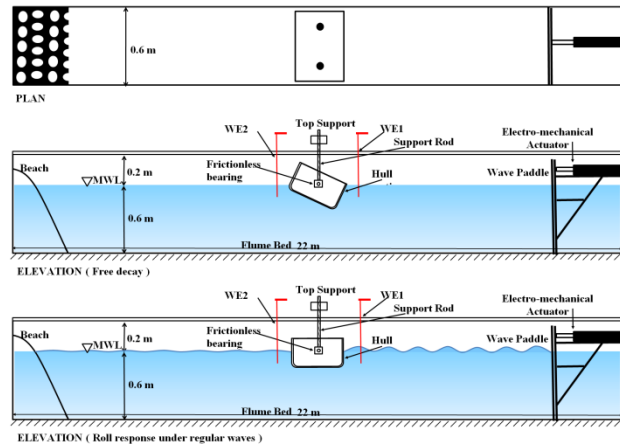
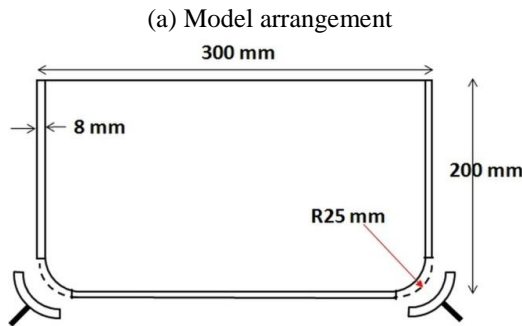
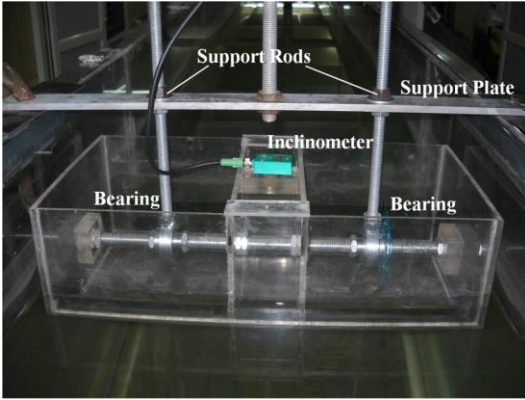


Figure 1: Experimental setup in glass flume

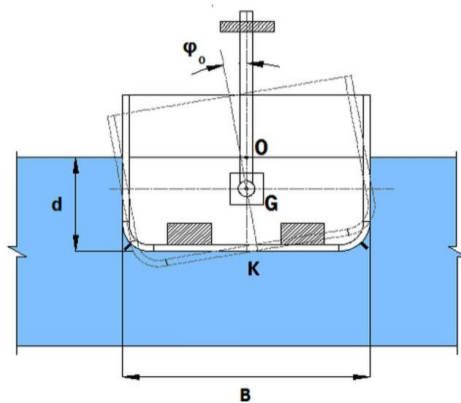
2.2 SHIP MODEL DETAILS

The prototype ship dimension considered has a width of 30 m and depth of 20 m with an overall length of 275 m with a draft 12 m. Typical Panamax ships of 100,000 ton displacement will have similar dimensions. The transverse dimensions of scaled model (1:100), are 300 mm in width (i.e. beam, B) and 200 mm in depth (D), i.e. a beam (B) to depth (D) ratio of 1.5. The model is fabricated to the almost full width of the wave flume (580 mm) with a small gap with flume wall that allows free rotation. It is made of 8 mm thick perspex sheets and its ends are closed to make it watertight. To achieve the required mass and vertical location of the centre of gravity (G), additional weights are placed inside the model hull at appropriate locations. The free rolling ball bearing is inserted on to the central longitudinal screw of the model along roll axis and it is

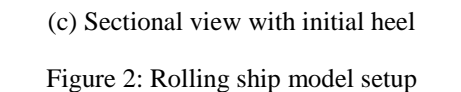
hung from the top railings of the wave flume. The ball bearing has been selected with minimum frictional resistance and is lubricated sufficiently for free rolling. The arrangement and sectional view of the model are shown in Fig. 2.



(a) Model arrangement



(b) Sectional view with dimensions



(c) Sectional view with initial heel

Figure 2: Rolling ship model setup

The point in the mean water surface on the vertical axis of symmetry of the model is taken as O and the point on this

axis at the keel is taken as K. The model was ballasted to a draft of $d = 0.12$ m.

The bilge radius of the model is 25 mm and this corresponds to a ship bilge radius (R) of 2.5 m. The experimental investigation is carried out for two configurations defined a BK00 and BK10 shown in Fig. 3 and described in Table 1. BK00 is the model without bilge keel and BK10 is model attached with 10 mm wide(b) bilge keel to the bilge inclined at 45° to the horizontal. The detailed inertia and hydrostatic properties of model is summarised in Table 2. The change in inertia for the model when attached with bilge keel will be considered in the calculations although; it is less than 2%. The VCG of the hull, with and without ballast, was determined by inclining experiment. The moment of inertia about the roll axis was calculated using a solid modeler (SOLIDWORKS) code using the geometry and location of the weights.

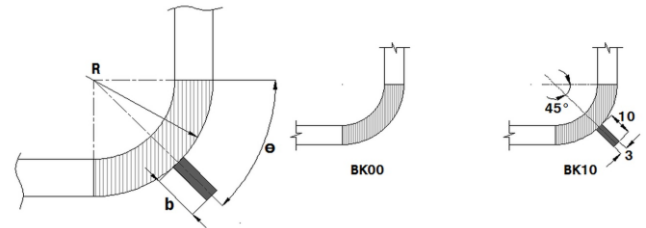


Figure 3: Bilge keel details

Table 1: Bilge keel dimensions and orientations

Bilge keel dimensions	BK00	BK10
Width (b) in mm	0	10
Width to Beam ratio (b/B)	0	0.033
Angle with horizontal (θ)	-	45°

Table 2: Hydrostatic and inertial properties of the ship model without bilge keel

Details	Values
Draft (d) (m)	0.12 m
Depth to Draft ratio (D/d)	1.67
Displacement (Δ)	20.88 kg
I	0.2244 kg-m ²
K_{xx}/B	0.346
BM	0.0625 m
KG	0.08 m
GM	0.0425 m

2.3 FREE ROLL DECAY AND ROLL RESPONSE OF SHIP MODEL UNDER REGULAR WAVES

The free roll decay test in calm water was conducted by giving an initial heel angle (ϕ_0) of 20° to the model (see Fig.1) to determine the roll natural period and damping.

The roll response experiment of the ship model with and without bilge keel under regular waves was carried out for a wave height of 3 cm and wave periods of 0.75 s to 2 s at the interval of 0.125 s. The model was also subjected to waves at its natural period to determine the maximum response it would attain at resonance.

The roll damping of the ship hull section was determined using logarithmic decrement method using the first five peaks of the roll decay curve. The damping ratio and natural frequency are obtained from the logarithmic decrement method using the following equations:

$$\delta = \ln \frac{\varphi_1}{\varphi_2} = \frac{2\pi\zeta}{\sqrt{1-\zeta^2}} ; \zeta = \frac{1}{\sqrt{1+\left(\frac{2\pi}{\delta}\right)^2}} \quad (1)$$

$$T_n = dT\sqrt{1-\zeta^2} \quad (2)$$

where δ is the logarithmic decrement, φ_1 and φ_2 are the two successive roll amplitudes, ζ is the roll damping ratio, T_n is the roll natural period and dT is the time difference between two successive roll amplitudes.

The equation of motion of the ship model for free roll decay is given by:

$$(I + A)\ddot{\varphi} + B(\dot{\varphi})\dot{\varphi} + C(\varphi)\varphi = 0 \quad (3)$$

where I is roll moment of inertia, B is nonlinear roll damping coefficient and C is the restoring moment (stiffness) coefficient, A is the added mass moment of inertia in roll and φ is the roll angle.

The equation of motion of the ship model under regular beam waves at zero forward speed is given by:

$$(I + A)\ddot{\varphi} + B(\dot{\varphi})\dot{\varphi} + C(\varphi)\varphi = M_0 \cos(\omega t - \alpha) \quad (4)$$

where M_0 is the wave excitation moment, ω is the wave frequency and α is the phase angle between the roll response and the wave excitation.

The roll RAO was determined by dividing the roll amplitude by the incident wave height of the regular wave. The experiments were repeated for three time to check the repeatability of the experiments. The error analysis is shown in Table 3, which shows the a negligibly small variance.

Table 3: Statistical variation of measured Peak RAO for BK00 and BK10 for H = 3 cm

d = 0.12 m	BK00	BK10
Test 1	20.749	9.569
Test 2	20.956	9.356
Test 3	20.57	9.823
Mean	20.758	9.583
Std. Dev.	0.158	0.191
Variance	0.025	0.036

3. CFD SIMULATION

Numerical wave tank (NWT) is a relatively new technique incorporating the viscous effects, wave hydrodynamics and floating body response. This procedure eliminates the assumptions made in the potential flow simulation in which the damping due to viscous effects are not included. The numerical wave tank includes the domain, floating body and end boundary conditions. The NWT simulated in the present study has the same dimensions of the wave flume except that the distance to the boundary on either side of the floating body is limited to avoid excessive computation time.

The CFD solver used in 2D numerical simulations of the experiments uses the Fractional Area/Volume Obstacle Representation (FAVOR) technique. This technique represents the body by calculating open area fractions on cell faces and open volume fractions in rectangular structured cells and distributing the solid and fluid portions in the cell. The cell size should be small enough to capture the complex geometries involving curved surfaces and thin plate like attachments such as the bilge keel. The dynamic fluid-structure interaction is solved with general moving objects (GMO) model which uses a fixed mesh technique as described by Wei[16]. The numerical ship model was allowed to roll about a fixed axis passing through its roll centre to replicate the experiments. The code can solve the multiphase flows involving free surface at the air-water interface using the volume of fluid (VOF) method. It also has an additional facility to silence the calculations for one of the phases which is of lesser importance for the flow problem. For the present simulation, the calculation for air phase is made silent and uniform atmospheric pressure is specified at the free surface. The $k-\varepsilon$ turbulence model was used in all calculations. An automatic variable time-stepping scheme based on the convergence and stability of the solution was used.

3.1 FREE ROLL DECAY SIMULATION

The free roll decay was simulated by inclining the model to specified initial heel angle, φ_0 as shown in Fig. 4(a). It also shows the domain extents and mesh details used for free roll decay simulation. The geometry initialized with fluid depth, initial heel and boundary conditions is shown in Fig. 5(a). The bottom boundary is wall, either side of the model is non-reflecting outflow and top is open to atmosphere with constant atmospheric pressure of 101325 Pa at free surface. The outflow boundaries are at distance of 6 m each from the centre of gravity of model on either side.

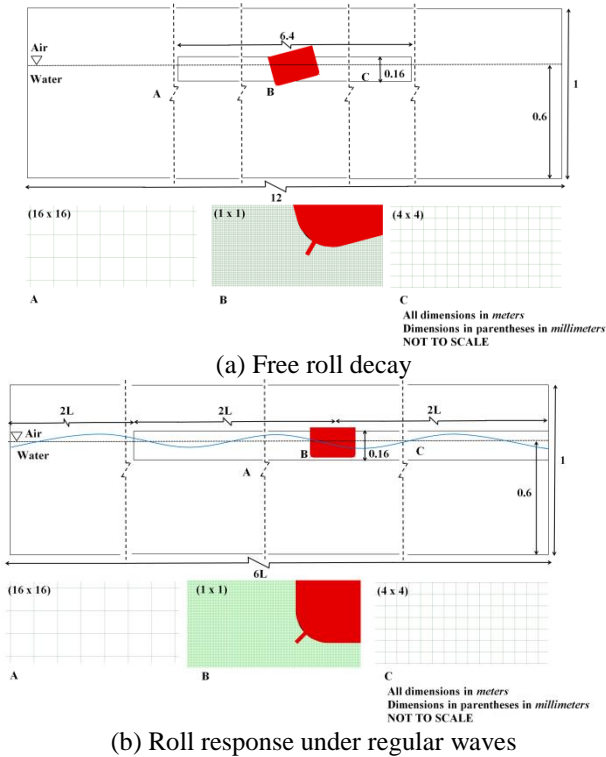


Figure 4: The computational domain (NWT)

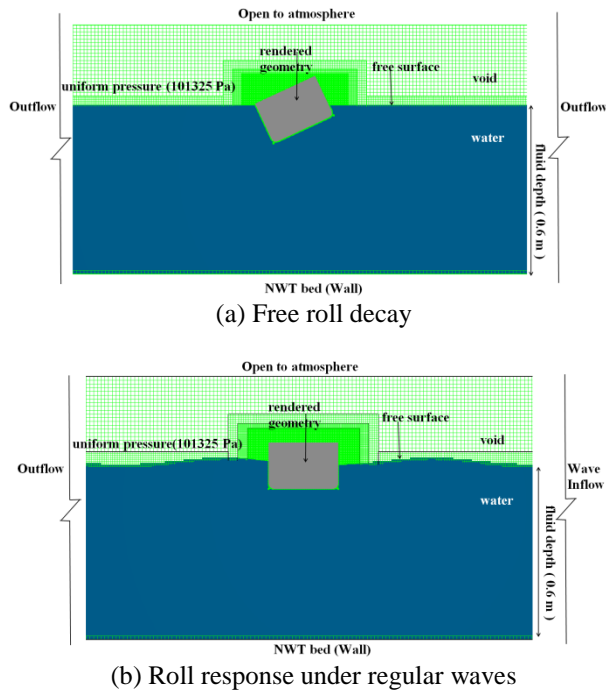


Figure 5: Geometry with initialised fluid for free roll decay and roll response simulation.

3.2 ROLL RESPONSE SIMULATION UNDER REGULAR WAVES

The simulation of roll response under regular waves was carried out with the similar boundary conditions except one of the outflow was set as regular wave inflow and the model was not given any initial heel. The wave inlet is located at distance of twice the wavelength ($2L$) from the model and the outflow boundary is located at distance of four times the wavelength ($4L$) from the model as shown in Fig. 4(b) with the mesh details. The waves of height 3 cm, at natural period and wave-periods ranging from 0.75 s to 2 s at the interval of 0.25 s were simulated. The domain initialised with a wave along with the boundary conditions is shown in Fig. 5 (b). The mesh near the model geometry (bilge curvature and bilge keel) and free surface is made finer for better resolution.

The mesh near the model is 1 mm x 1 mm and in the free surface it is 4 mm x 4 mm (see zoomed view of Fig. 4(a) and 4(b)). The air phase is defined as void for both free roll decay simulation and roll response simulation under regular waves.

4. RESULTS AND DISCUSSION

4.1 VALIDATION OF CFD WITH EXPERIMENTS

The comparison of the measured and simulated free roll decay for BK00 and BK10, inclined at $\phi_0 = 20^\circ$ is shown in Fig. 6(a) and 6(b) respectively. Similarly, the comparison of the measured and simulated roll response under a regular wave of height 3 cm and their respective natural periods is shown in Fig. 7(a) for BK00 and in 7(b) for BK10. It can be seen that there is a close comparison between the measured and simulated responses.

Table 4: Comparison of measured and simulated damping ratio (ζ) and natural roll period (T_n) for $\phi_0 = 20^\circ$

Bilge keel	CFD		Expt.	
	ζ	T_n	ζ	T_n
BK00	0.031	1.109	0.033	1.114
BK10	0.076	1.159	0.075	1.196

4.2 EFFECT OF BILGE KEEL ON ROLL DAMPING AND ROLL NATURAL PERIOD

The attachment of bilge keel (BK10) increases the roll damping and the roll natural period of the model. The increase in the roll damping for BK10 is mainly due to the forces acting on the bilge keel. The normal force on the bilge keel surface and the pressure variation around the hull with the presence of bilge keel cause the ship model motion to damp faster. The pressure variation around the hull is caused because of the flow separation and stronger

vortex formation from the bilge keel. The vorticity plots for BK00 and BK10 in free roll decay inclined at $\phi_0 = 20^\circ$ is shown Fig. 8 and Fig. 9 respectively. The vorticity contours are plotted against the ratio of instantaneous time (t) to natural period of model (T_n). BK10 exhibits a stronger vortex shedding compared with BK00 causing increase in roll damping. The increase in damping ratio for BK10 compared with BK00 is about 127.3% as can be seen in Table 4. The roll natural period of the model is increased for BK10 as compared to BK00. BK10 has increased hydrodynamic added mass with the presence of bilge keel. This increases the effective moment of inertia along the roll axis of the model which shifts the natural period. The increase in roll natural period is about 7.4% with the attachment of bilge keel (Table 4).

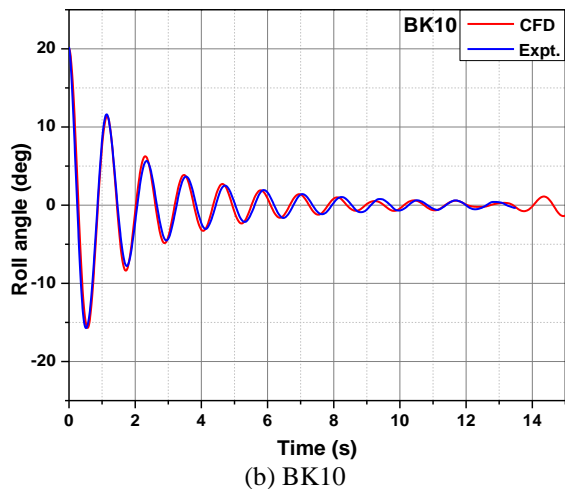
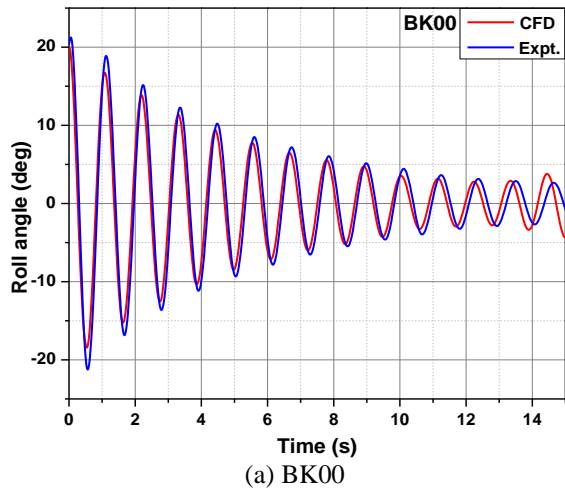


Figure 6: Comparison of measured and simulated free roll decay for $\phi_0 = 20^\circ$

4.3 EFFECT OF BILGE KEEL OF ROLL RESPONSE

The measured and simulated roll response of the ship model shown in Fig. 7 exhibit a considerable reduction in

the resonant roll response for BK10 as opposed to BK00 (also see Fig. 10). The increase in the roll damping with attachment of bilge keel has a significant effect in reducing roll response.

There is obvious shift of the peak roll RAO for BK10 due to increase in natural period as discussed earlier. The inertia dominant region i.e. towards the left of the peak RAO and the damping dominant region (near peak RAO) show a reduced response for BK10 in comparison with BK00. And in the stiffness dominant region toward the right of the peak RAO the responses for BK10 and BK00 are similar. The reduction in the peak RAO in deg/cm of wave height (H) from BK00 to BK10 is about 53.8% as can be seen in Table 3 and Fig. 10. The roll RAO for BK00 at its resonance is very high due to a lesser damping and the model being allowed only to roll, restricting the other degrees of freedom.

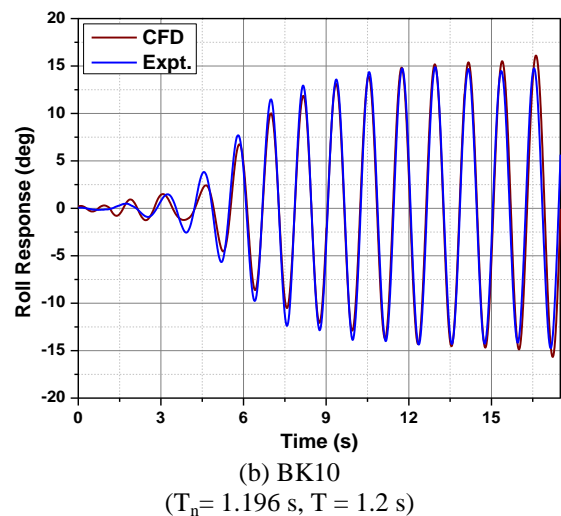
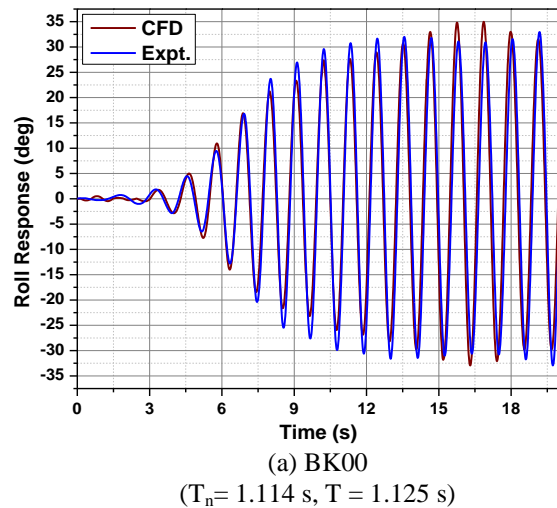


Figure 7: Comparison of measured and simulated roll response under regular waves near natural periods for $H = 3$ cm

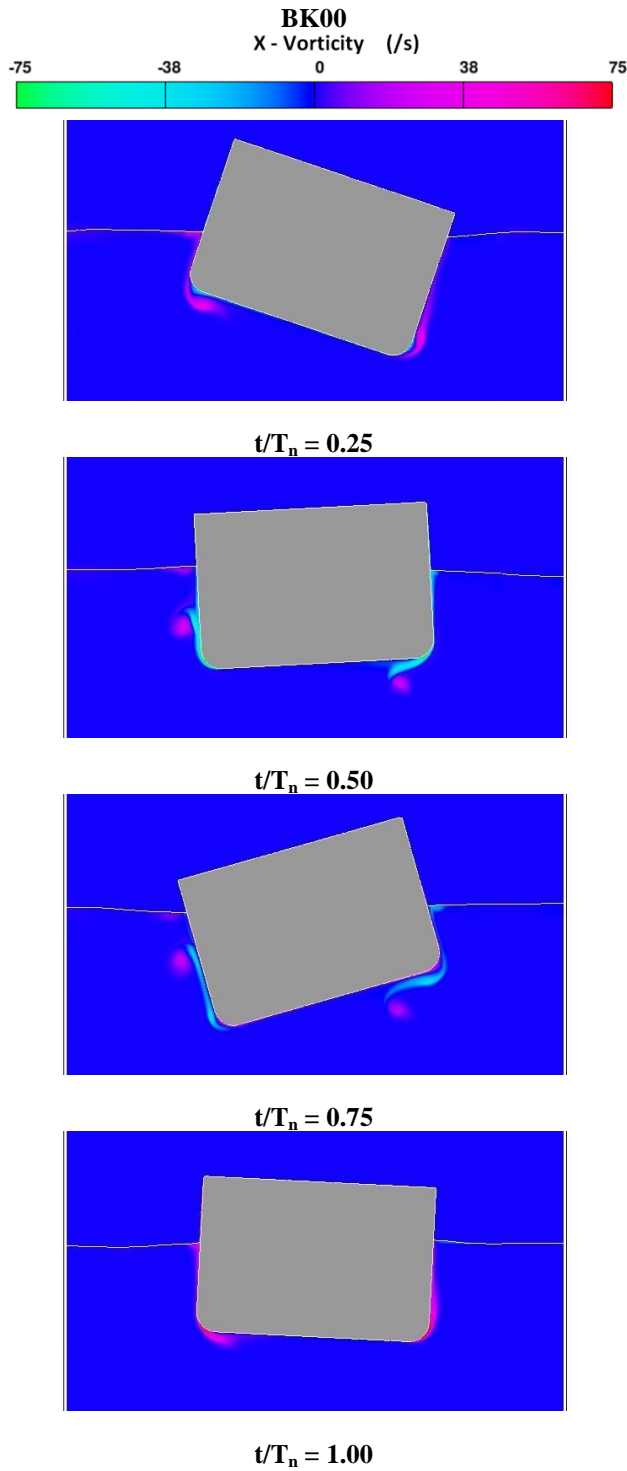


Figure 8: Comparison vorticity contours for BK00 and in free roll decay at $\phi_0 = 20^\circ$

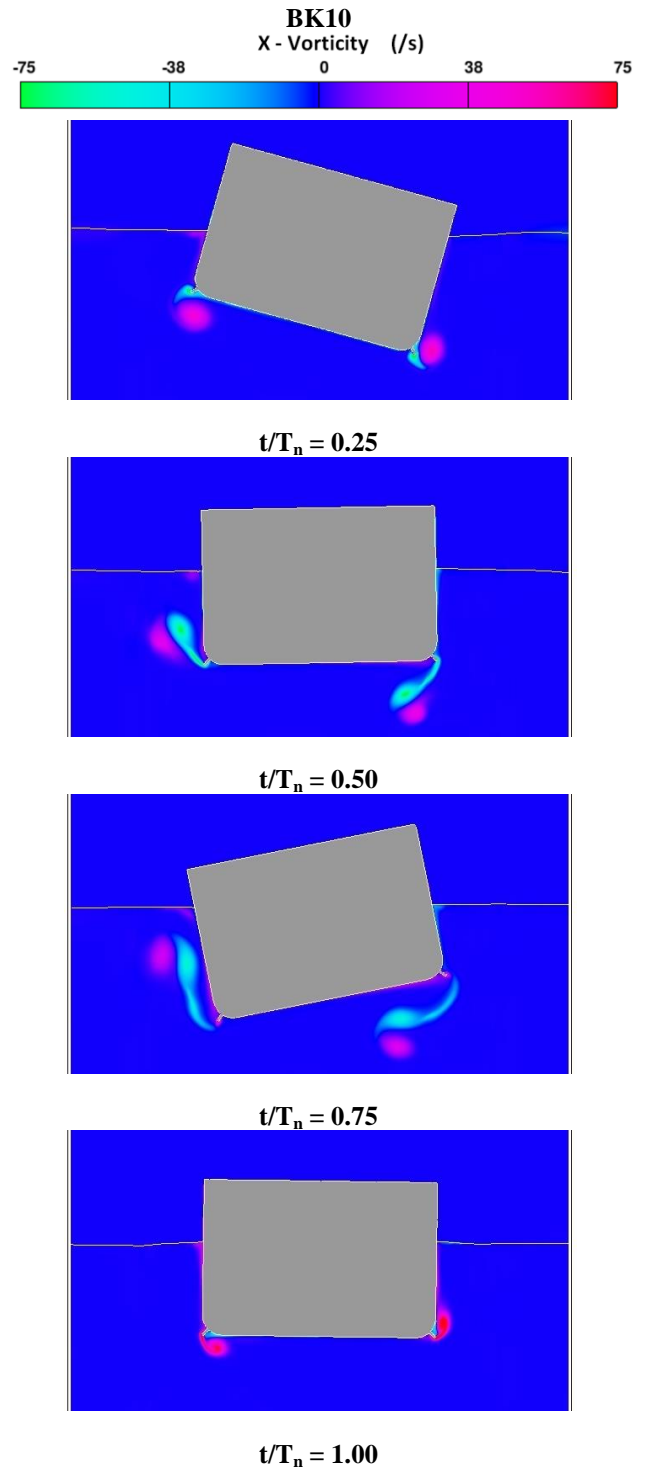


Figure 9: Comparison vorticity contours for BK10 and in free roll decay at $\phi_0 = 20^\circ$

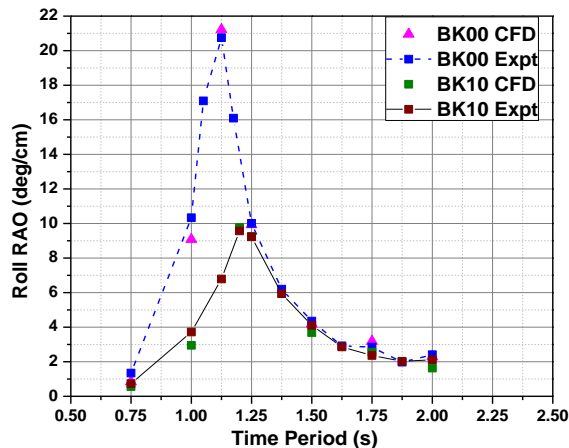


Figure 10: Comparison of measured and simulated roll RAO under regular waves for $H = 3$ cm

5. CONCLUSIONS

The effectiveness of bilge keel in improvement of roll damping was studied by conducting experiments on ship model section. The experimental output was used to validate the commercial CFD code. Attachment of bilge keel to the hull section of the ship model improved the roll damping to a significant value and this was very closely replicated in the CFD simulations. The roll response at resonance was reduced to half when compared with the model having no bilge keel. The measured roll RAO compared with that from the CFD simulation show a very good agreement. Thus, CFD with the facility of NWT can be used efficiently to simulate the non-linear motions of floating bodies arising from viscous effects. This rules out the use of simplified empirical or semi-empirical formulae for prediction of such motions.

6. ACKNOWLEDGEMENTS

The authors would like to thank the Naval Research Board, Government of India, for financial support.

7. REFERENCES

1. IKEDA, Y., HIMENO, Y. & TANAKA, N., 'On Eddy Making Component of Roll Damping Force on Naked Hull.', *J. Soc. Nav. Archit. Japan* **142**, (1977).
2. IKEDA., Y., KOMATSU, K., HIMENO, Y. & TANAKA, N., 'On Roll Damping Force of Ship- Effect of Hull Surface Pressure Created By Bilge Keels.', *J. Kansai Soc. Nav. Archit. Japan* **165**, (1977).
3. IKEDA., Y., HIMENO, Y. & TANAKA, N., 'Components of Roll Damping of Ship at Forward Speed.', *J. Soc. Nav. Archit. Japan* **143**, (1978).

4. SCHMITKE, R. T., 'Ship Sway, Roll, and Yaw Motions in Oblique Seas.', *SNAME Trans.* **86**, 26–46 (1978).

5. HIMENO, Y. 'Prediction of Ship Roll Damping- State Of Art.', *Report of Department of Naval Architecture and Marine Engineering, No. 239, University of Michigan.* (1981).

6. CHAKRABARTI, S., 'Empirical calculation of roll damping for ships and barges.', *Ocean Eng.* **28**, 915–932 (2001).

7. KAWAHARA, Y., MAEKAWA, K. & IKEDA., Y., 'A simple prediction formula of roll damping of conventional cargo ship by Ikeda method and limitations.', *J. Shipp. Ocean Eng.* **2**, 201–210 (2012).

8. BRYAN, G. H., 'The Action of Bilge Keels.' *Trans. Inst. Nav. Archit.* **42**, (1900).

9. RODDIER, D., LIAO, S. & YEUNG, R. W., 'Wave-Induced Motion of Floating Cylinders Fitted with Bilge Keels.', *Int. J. Offshore Polar Eng.* **10**, 241–248 (2000).

10. SEAH, R. K. M. & YEUNG, R. W., 'Sway and Roll Hydrodynamics of Cylindrical Sections.', *Int. J. Offshore Polar Eng.* **13**, 241–248 (2003).

11. NA, J. H., LEE, W. C., SHIN, H. S. & PARK, I. K., 'A Design of Bilge Keels for Harsh Environment FPSOs.', in *Proc. Twelfth Int. Offshore Polar Engineering Conf.* **3**, 114–117 (2002).

12. YU, Y., KINNAS, S. A., VINAYAN, V. & KACHAM, B. K., 'Modeling of Flow around FPSO Hull Sections Subject to Roll Motions : Effect of the Separated Flow around Bilge Keels.', in *Proc. Fifteenth Int. Offshore Polar Eng. Conf.* **8**, 163–170 (2005).

13. YU, Y. H. & KINNAS, S. A., 'Roll Response of Various Hull Sectional Shapes Using a Navier-Stokes Solver.', *Int. J. Ocean Syst. Eng.* **19**, 46–51 (2009).

14. BANGUN, E. P., WANG, C. M. & UTSUNOMIYA, T., 'Hydrodynamic forces on a rolling barge with bilge keels.', *Appl. Ocean Res.* **32**, 219–232 (2010).

15. THIAGARAJAN, K. P. & BRADDOCK, E. C., 'Influence of Bilge Keel Width on the Roll Damping of FPSO.', *J. Offshore Mech. Arct. Eng.* **132**, 011303 (2010).

16. **WEI, G.**, 'A Fixed-mesh Method for General Moving Objects in Fluid Flow.', *Int. J. Mod. Phys. B* **19**, 1–4 (2005).

8. AUTHORS BIOGRAPHY

Irkal Mohsin A. R. is a research scholar at the Department of Ocean Engineering, Indian Institute of Technology Madras, Chennai - 600036 (Email: irkal.mohsin@gmail.com)

S. Nallayarasu is a Professor at the Department of Ocean Engineering, Indian Institute of Technology Madras, Chennai - 600036 (Email: nallay@iitm.ac.in)

S. K. Bhattacharyya is a Professor at the Department of Ocean Engineering, Indian Institute of Technology Madras, Chennai - 600036 (Email: skbh@iitm.ac.in)